Lane J. Jaeckle Santos,[1,2] Changhong Li,[1,2] Paschalis-Thomas Doulias,[2] Harry Ischiropoulos,[1,2] G. Scott Worthen,[1,2] and Rebecca A. Simmons[1,2]

Neutralizing Th2 Inflammation in Neonatal Islets Prevents β-Cell Failure in Adult IUGR Rats

Intrauterine growth restriction (IUGR) leads to development of type 2 diabetes (T2D) in adulthood. The mechanisms underlying this phenomenon have not been fully elucidated. Inflammation is associated with T2D; however, it is unknown whether inflammation is causal or secondary to the altered metabolic state. Here we show that the mechanism by which IUGR leads to the development of T2D in adulthood is via transient recruitment of T-helper 2 (Th) lymphocytes and macrophages in fetal islets resulting in localized inflammation. Although this immune response is short-lived, it results in a permanent reduction in islet vascularity and impaired insulin secretion. Neutralizing interleukin-4 antibody therapy given only in the newborn period ameliorates inflammation and restores vascularity and β-cell function into adulthood, demonstrating a novel role for Th2 immune responses in the induction and progression of T2D. In the neonatal stage, inflammation and vascular changes are reversible and may define an important developmental window for therapeutic intervention to prevent adult-onset diabetes.

Diabetes 2014;63:1672–1684 | DOI: 10.2337/db13-1226

ISLET STUDIES

Intrauterine growth restriction (IUGR) is a common complication of pregnancy and is linked to the later development of type 2 diabetes (T2D) (1,2). We have developed an experimental animal model of IUGR caused by uteroplacental insufficiency, which limits the supply of critical substrates and hormones to the fetus. This abnormal metabolic intrauterine milieu affects the development of the fetus by permanently altering susceptible cells, such as β-cells, and leads to the development of T2D in adulthood.

Inflammation is highly associated with T2D in a variety of studies and experimental models of T2D. In adult GK and spontaneously diabetic Torii rats, there is increased fibrosis (3,4) and evidence of inflammation in islets (5–7). However, it remains unknown whether inflammation is casual in the development of diabetes or merely associated with an existing metabolic disease state. Much of the characterization of inflammation in T2D models has occurred in adult diabetic or dysmetabolic animals, which makes dissecting the cause and effect of inflammation in diabetes difficult. Our model of IUGR is both relevant and unique to the study of human T2D because it allows us to characterize the role inflammation plays in the early events of T2D development, beginning in utero.

Key immune effector cells with links to T2D, inflammation, and metabolic syndrome are T-cells and tissue macrophages (8). T-helper (Th) cells play a pivotal role in amplifying immune responsiveness, which directly affects the activation and proliferation of tissue macrophages. Th cells are classified into several subsets, depending on the cytokines associated with their differentiation. One subset is Th2 cells, which can release interleukin (IL)-4 and stimulate an alternate activation of macrophages (M2), aiding in tissue repair and wound

[1]Division of Neonatology, Department of Pediatrics, Perelman School of Medicine, University of Pennsylvania, Philadelphia, PA
[2]The Children's Hospital of Philadelphia, Philadelphia, PA

Corresponding author: Rebecca A. Simmons, rsimmons@mail.med.upenn.edu, or G. Scott Worthen, worthen@email.chop.edu.

Received 9 August 2013 and accepted 26 December 2013.

This article contains Supplementary Data online at http://diabetes.diabetesjournals.org/lookup/suppl/doi:10.2337/db13-1226/-/DC1.

healing (9–12). While Th2 cytokines are often associated with anti-inflammatory effects, inflammation due to Th2 activation characterizes asthma, hypersensitivity, and allergies. To date, Th2 inflammation has not been linked to T2D pathogenesis.

Inflammation is present in islets of T2D patients with diabetes based on increased macrophage presence and cytokine release from islets. This inflammation is thought to be primarily the result of increased levels of the proinflammatory cytokine IL-1β, which initiates and amplifies proinflammatory responses (13,14). While IL-1β can affect many Th responses, the method of IL-1β inflammation is largely independent of T-cells. Early clinical trials targeting IL-1β show relatively mild decreases in hemoglobin A_{1c} and modestly increased insulin secretion, suggesting that IL-1β activation is but one of many immune pathways responsible for islet dysfunction in T2D (15–17).

In this study, we demonstrate that Th2-mediated immune inflammation begins in the fetal IUGR pancreas. This response results in the recruitment of tissue-remodeling macrophages and negatively affects islet vasculature and function months before diabetes develops. Neutralizing IL-4 levels in newborn IUGR animals ameliorates immune invasion, restores islet vascularity and function, and prevents hyperglycemia in adulthood, demonstrating a new role for Th2 inflammation in the pathogenesis of diabetes.

RESEARCH DESIGN AND METHODS

Animal Model

Our animal model has been previously described (18,19). Briefly, on day 18 of gestation (term is 22 days), pregnant rats were anesthetized with intraperitoneal xylazine (8 mg/kg) and ketamine (40 mg/kg), and both uterine arteries were ligated. Controls underwent sham surgery. Rats recovered within a few hours and had ad lib access to food and water. The pregnant rats were allowed to deliver spontaneously, and the litter size was randomly reduced to eight at birth to assure uniformity of litter size between IUGR and control litters. Measurements were made 24 h postsurgery at embryonic day 19 (e19), postnatal day (PD) 14, and 15 weeks. After PD14, female offspring were excluded, and only male animals were used. For fetal measurements, blood or isolated islets were pooled from all pups from a single litter. This is considered an *n* of 1. For postnatal measurements, blood or islets were collected from individual animals from different litters. For antibody treatment, animals were divided into four groups: control treated with PBS (control vehicle [CV]), IUGR treated with PBS (IUGR vehicle [IV]), control animals treated with neutralizing IL-4 antibodies (CIL4), and IUGR animals treated with neutralizing IL-4 antibodies (IIL4). These studies were approved by the Animal Care Committee of The Children's Hospital of Philadelphia.

Islet Isolation

Rat islets were isolated by ductal collagenase perfusion and Histopaque gradient separation (Sigma). Pancreata were perfused with Hanks' balanced salt solution supplemented with 1% BSA (wt/vol; Fisher), 4 mmol/L $NaHCO_3$ (Sigma), and 10 mg/mL Collagenase P (Roche); excised; and incubated at 37°C for 15–30 min. After digestion, islets were washed and then purified using a Histopaque discontinuous gradient (Sigma). For fetal islet isolation, collagenase concentration was decreased to 2 mg/mL and incubated at 37°C for 10 min.

RNA Extraction

Total RNA was isolated from pooled fetal islets (n = 4 different litters) and at 2 weeks (n = 4 different animals) using RNAzol B (Tel-Test). RNA from isolated islets was bioanalyzed for RNA integrity (Agilent) and samples with RNA integrity number scores less than 7.5 were excluded. Quantitative PCR was performed as previously described (20).

Microarray Analyses

cDNA was synthesized from RNA[17]. To measure differential gene expression in PD14 IUGR and controls, an Agilent two-color array was used. Differentially labeled IUGR and control RNA were hybridized to the same array, and a total of four arrays from four different sample pairings were analyzed. There was very little contamination of exocrine tissue in the islet preps. However, control and IUGR samples were paired based on similar expression levels of exocrine (amylase, chymotrypsin) and endocrine (insulin, glucagon) genes. RNA samples from the resulting four groups were amplified with WT-Ovation Pico (NuGEN Technologies). Amplified cDNA was labeled using BioPrime (Invitrogen) with Cy3/Cy5-labeled nucleotides (GE Amersham Biosciences). Labeled samples were hybridized overnight to the 4 × 44 Rat Gene Expression Microarray (Agilent) and scanned with a G2565B DNA microarray scanner (Agilent). The e19 microarray experimental design was a single color array from Affymetrix, and four individual samples each of IUGR and control RNA were analyzed. RNA samples from e19 were amplified with the WT Expression Kit (Ambion) and labeled with the GeneChip WT Terminal Labeling Kit (Affymetrix). Labeled samples were hybridized, washed, stained, and scanned using standard protocols for Rat Gene 1.0 ST (Affymetrix). Array .cel files were imported into Partek Genomics Suite (v6.6, Partek Inc., St. Louis, MO), where RNA normalization was applied. Transcript cluster identifications were filtered to exclude technical controls, and intersample variation was visualized using principal components analysis. To identify differentially expressed transcripts, data were exported to R where SAM [samr v2.0 (21)] was applied. Functional analyses for both arrays were generated using Interactive Pathway Analysis (Ingenuity Systems, www.ingenuity.com). Complete microarray data are publically available through the

National Institutes of Health Gene Expression Omnibus database (www.ncbi.nlm.nih.gov/geo/): e19 microarray accession GSE48655 and PD14 microarray accession GSE48822.

Cytokine and Hormone Measurements

Blood was collected and allowed to clot for 2 h at room temperature. Serum was isolated by centrifugation at 10,000*g* for 10 min and frozen. Islets (n = 6–8 per group) were isolated, and tissue was resuspended in 1 × PBS (vol/vol) with 0.1% Triton-X 100 (vol/vol; Integra), 1% Protease Inhibitor Cocktail (vol/vol; Sigma), and 1% Phosphatase Inhibitor Cocktail (vol/vol; Sigma). Tissues were homogenized and centrifuged for 10 min at 10,000*g*. Lysate samples were normalized to total protein concentration as measured by BCA Assay (Pierce). Insulin was measured by Ultra Sensitive ELISA (Mercodia), and C-peptide was measured by ELISA (ALPCO). Cytokine and chemokine panels were measured by Luminex Assay (EMD Millipore).

Histology

Excised tissues were placed in formalin-free zinc fixative (BD Pharmingen) for 24–48 h and embedded in paraffin. CD3 antibody (BD Pharmingen), CD68 antibody (Abcam), insulin antibody (Abcam), and biotinylated *Griffonia* (*Bandeiraea*) *simplicifolia* lectin I (Vector Laboratories B1105) was used to stain zinc-fixed, paraffin-embedded tissue. Slides were incubated with CD3 antibody at a 1:100 overnight at 4°C, CD68 antibody at a 1:100 for 1 h at room temperature, insulin antibody at a 1:500 overnight at 4°C, or biotinylated lectin at a 1:5,000 overnight at 4°C. For capillary density quantification, lectin staining intensity was quantified as a percentage of islet area as previously described (22). For β-cell mass measurements, a minimum of four sections separated by at least 200 μm were chosen, stained for insulin, and then scanned with Aperio Scan Scope OS. Images were analyzed using Aperio Image Analysis v11.1.2.760 Toolkit algorithms Genie Classifier v1 and Color Deconvolution v9. Results were expressed as a percentage of insulin-positive area relative to the total area scanned. Total β-cell mass was calculated by normalizing β-cell percentage to total pancreas weight.

Microscopy Slides

Images were captured on a Leica DMRBE microscope with 40× magnification (PL Fluotar 40×/0.70) and QImaging Micropublisher 5.0 RTV camera. iVision software version 4.0.16 was used for acquisition, and images were processed for size, color balance, brightness, and contrast using ImageJ version 1.46r.

Nuclear Magnetic Resonance Scanning

At PD14, body composition was measured in animals from the four treatment groups using nuclear magnetic resonance spectroscopy (Echo MRI) (23). The percentage of fat and lean tissue per animal was calculated per gram of total body weight.

Neutralizing IL-4 Therapy

Control and IUGR animals were injected subcutaneously with 1 μg/kg of purified mouse antirat IL-4 antibody (BD Pharmingen), mouse isotype control IgG1κ (BD Pharmingen), or PBS (Fisher BioReagents) daily from PD1–6.

Insulin Secretion by Perifused Islets

In brief, islets were isolated by collagenase digestion and cultured with 10 mmol/L glucose in RPMI 1640 medium (Sigma) for 3 days. One hundred cultured rat islets were loaded onto nylon filters in a small chamber and perifused in a Krebs-Ringer bicarbonate buffer with 0.25% BSA at a flow rate of 2 mL/min. Perifusate solutions were gassed with 95% O_2/5% CO_2 and maintained at 37°C. Islets were perifused in glucose-free solution with 2 mmol/L glutamine (used as an alternate fuel source), then glucose concentrations were increased at a rate of 0.625 mmol/L glucose/min to a final concentration of 25 mmol/L. Samples were collected every minute and used to measure insulin by homogeneous time resolved fluorescence (Cisbio).

Measurement of Nitric Oxide Metabolites

Protein from islet lysates was removed using Ultracel 3,000 centrifugal filters according to manufacturer instructions (Millipore). Nitric oxide (NO) metabolites were evaluated by reducing metabolites, using acidified-heated vanadium, to NO; NO was detected via chemiluminescence on a Sievers 280 NO analyzer. Samples were injected into a custom-made purge container containing 0.05 mol/L vanadium chloride in 1 N HCl heated to 95°C. The reading in millivolts was compared with a standard curve generated by injecting standard solutions of nitrate. This reductive method provides information about the total levels of nitrate, nitrite, N-nitroso, and iron-nitrosyl adducts as well as low-molecular-weight and protein S-nitrosothiol adducts.

Measurement of Lipid Peroxidation

Islet lysates were analyzed for lipid peroxidation using the Parameter TBARS kit (R&D Systems) according to manufacturer instructions and normalized to protein content.

Statistical Analysis

Data points were analyzed for normal distribution, and transformed if necessary, then tested for statistical significance using Student t test and an α of 0.05. If normal distribution could not be determined, analysis by nonparametric Mann-Whitney test was performed.

RESULTS

Gene Expression in IUGR Islets Shows Immune Inflammation

We assessed global mRNA expression profiles by microarray analysis in IUGR islets at e19, 24 h after induction of surgery. In IUGR islets, 1,220 genes were upregulated

and 1,090 were downregulated at least 1.5-fold compared with controls filtered on a false discovery rate (FDR) of 10% (Table 1).

Ingenuity analysis identified pathways involved in activation of macrophages, immune cell trafficking and inflammatory response ($P = 2.95 \times 10^{-7}$), and complement activation ($P = 9.46 \times 10^{-7}$). Analysis of expression of individual immune-related genes suggested activation of CD4-positive Th cells in IUGR islets, with two distinct groups of genes: the activation of those that promote or enhance a Th2 cell response and macrophage activation and the downregulation of genes that promote an alternate Th lineage, Th1. Th1 and Th2 responses are antagonistic, and the downregulation of Th1 genes further activates a Th2 response.

The complement system is involved in the sensing and clearing of injured cells and plays a significant role in the pathogenesis of various inflammatory responses (24). In IUGR e19 islets, genes regulating complement alternative pathway were upregulated. Activation of C3 through the alternate pathway is necessary for IL-4 production in some diseases of dysregulated Th2 activation such as asthma (25,26).

Ingenuity analysis of the gene list also revealed activation of genes involved in digestive system development and function ($P = 3.99 \times 10^{-6}$). Transcription factors critical to normal pancreatic and β-cell function and development were upregulated, many of which directly regulate insulin production through interactions at the insulin promoter. These results suggest a compensatory mechanism in fetal IUGR islets in response to nutrient deprivation.

We next assessed global mRNA expression profiles by microarray analysis in IUGR islets at PD14. In IUGR islets, 15 genes were upregulated and 252 were downregulated compared with controls filtered on an FDR of 10% (Table 2). Ingenuity analysis revealed several pathways that were enriched in IUGR islets, including inflammatory response ($P = 7.87 \times 10^{-7}$), cellular movement ($P = 2.02 \times 10^{-7}$), tissue development ($P = 1.81 \times 10^{-6}$), cardiovascular system development and function ($P = 1.91 \times 10^{-6}$), and connective tissue development and function ($P = 1.32 \times 10^{-5}$). Analysis of individual immune-related genes continued to show altered expression of genes involved in the promotion of a Th2 immune response and M2 macrophage activation. M2 macrophage activation is critical to the propagation of a Th2 response (10), and consistent with a Th2 response activation, genes that prevent monocyte differentiation into M2 macrophages were downregulated.

Many proangiogenic genes were dysregulated in IUGR islets, and their downregulation is consistent with decreased vascular endothelial growth factor (VEGF) levels and diminished vascularity that we have previously observed in IUGR islets (22). We confirmed expression patterns for selected genes from both e19 and PD14 arrays (Supplementary Table 1).

Fetal IUGR Islets Show Localized Th2 Immune Response

To further characterize immune activation in IUGR animals, we measured a panel of inflammatory cytokines and chemokines in serum and isolated islet lysate. The panel was enriched for both Th1 and Th2 immune responses and cytokines associated with T2D and insulin resistance. Cytokine profiling was assessed at e19 in serum and isolated islet lysate (Fig. 1*A* and *B*, Supplementary Table 1), which allows characterization of both systemic (serum) and localized (islet lysate) responses as the IUGR animal progresses toward the eventual development of diabetes. We observed a 78% decrease in circulating leptin and a 62% decrease in insulin compared with controls. Fetal leptin and insulin levels have been shown to mirror fetal growth in cord blood from small for gestational age neonates (27,28), which is consistent with the decline in growth seen in this experimental model. Insulin levels in fetal islet lysates were unchanged (Fig. 1*B*). These results confirm the previously demonstrated (18) insulin secretory defect within 24 h of surgery. IL-4, IL-2, eotaxin, and IL-10 were all increased more than twofold in fetal islet lysates but were undetectable in fetal serum from either group, suggesting that IUGR induces an islet-specific localized inflammatory response. Th lymphocyte subpopulations are defined by the cytokines released, and all four elevated cytokines present in islet lysate (IL-4, IL-2, IL-10, and eotaxin) are consistent with a Th2 response. The proinflammatory cytokines RANTES (regulated on activation, normal T-cell expressed and secreted) and monocyte chemoattractant protein (MCP) 1 were elevated by 30 and 45% in lysates, respectively. MCP1 (CCL2) is the primary stimulant for monocyte and macrophage recruitment and overexpression results in insulin resistance in rodents (29). Elevated IL-4 levels in e19 lysates were independently confirmed by ELISA (Supplementary Table 1).

Postnatal IUGR Animals Have Systemic and Islet Inflammation

At PD14, there was a 2.7-fold increase in serum leptin levels in IUGR compared with controls (Fig. 1*C*, Supplementary Table 1), correlating with a previously observed increase in adiposity in IUGR animals, despite reduced total body weight at 2 weeks of age (30). High leptin levels have been shown to inhibit β-cell growth through AKT signaling pathways (31). Circulating levels of insulin were elevated 2.8-fold compared with controls, consistent with insulin resistance. The proinflammatory cytokines MCP1 and RANTES were both significantly increased more than threefold in serum. These cytokines were unchanged or undetectable in fetal serum, demonstrating that sustained systemic inflammation likely develops after birth.

By PD14, islet lysates continued to show increased immune cytokines and localized inflammation, with IL-2

Table 1—e19 IUGR islets show increases in immune and macrophage activating genes

Gene	Description	Fold Change	FDR	Function
Activation and migration of macrophages				
A2M	α-2 macroglobulin	6.7	2.9	Promote Th2/M2 macrophages
PZP	Pregnancy-zone protein	5.4	3.6	Promote Th2/M2 macrophages
F2	Coagulation factor II (thrombin)	4.0	4.8	Promote Th2/M2 macrophages
PPARA	Peroxisome proliferator activated receptor α	3.7	2.4	Promote Th2/M2 macrophages
SERPINF2	Serine (or cysteine) peptidase inhibitor, clade F, member 2	3.6	4.8	Promote Th2/M2 macrophages
HDC	Histidine decarboxylase	3.5	3.6	Promote Th2/M2 macrophages
PLG	Plasminogen	3.2	4.8	Promote Th2/M2 macrophages
AGT	Angiotensinogen	3.1	2.9	Promote Th2/M2 macrophages
PROC	Protein C	3.0	4.1	Promote Th2/M2 macrophages
TFF2	Trefoil factor 2	2.8	4.8	Promote Th2/M2 macrophages
ITGB6	Integrin, β 6	2.8	0.4	Promote Th2/M2 macrophages
CCL9	Chemokine (C-C motif) ligand 9	2.7	4.8	Promote Th2/M2 macrophages
F10	Coagulation factor X	2.7	9.8	Promote Th2/M2 macrophages
IRF6	Interferon regulatory factor 6	2.6	1.7	Promote Th2/M2 macrophages
HSPB8	Heat shock protein B8	2.5	0.4	Promote Th2/M2 macrophages
F2RL1	Coagulation factor II (thrombin) receptor-like 1	2.4	1.5	Promote Th2/M2 macrophages
F5	Coagulation factor V (proaccelerin, labile factor)	2.3	9.8	Promote Th2/M2 macrophages
IL1RN	IL-1 receptor antagonist	2.3	5.6	Promote Th2/M2 macrophages
GC	Group specific component	2.3	3.2	Promote Th2/M2 macrophages
MET	Met proto-oncogene	2.3	1.6	Promote Th2/M2 macrophages
CBS	Cystathionine β synthase	2.2	2.9	Promote Th2/M2 macrophages
F3	Coagulation factor III	2.1	1.4	Promote Th2/M2 macrophages
PTGES	Prostaglandin E synthase	2.1	1.3	Promote Th2/M2 macrophages
NDRG1	N-myc downstream regulated gene 1	2.1	1.6	Promote Th2/M2 macrophages
LAMA5	Laminin, α 5	2.1	0.8	Promote Th2/M2 macrophages
ARG1	Arginase, liver	1.8	9.8	Promote Th2/M2 macrophages
KLRK1	Killer cell lectin-like receptor subfamily K, member 1	−2.8	9.8	Promote Th1/M1 macrophages
FCGR1A	Fc fragment of IgG, receptor (CD64)	−2.7	6.6	Promote Th1/M1 macrophages
SNCA	Synuclein, α	−2.6	6.6	Promote Th1/M1 macrophages
CX3CR1	Chemokine (C-X3-C motif) receptor 1	−2.5	9.8	Promote Th1/M1 macrophages
CD79B	Cd79b molecule	−2.4	9.8	Promote Th1/M1 macrophages
CD180	CD180 molecule	−2.4	9.8	Promote Th1/M1 macrophages
CORO1A	Coronin, actin binding protein 1A	−2.2	9.8	Promote Th1/M1 macrophages
CD7	CD7 molecule	−2.1	6.6	Promote Th1/M1 macrophages
CD200	CD200 molecule	−2.1	9.8	Promote Th1/M1 macrophages
RHOH	ras Homolog gene family, member H	−2.1	9.8	Promote Th1/M1 macrophages
TLR7	Toll-like receptor 7	−2.0	9.8	Promote Th1/M1 macrophages
Embryonic organ development and endocrine system development and function				
ACVR1C	Activin A receptor, type IC	2.0	1.6	—
ALDOB	Aldolase B, fructose-bisphosphate	2.2	2.4	—
BCL2L14	Bcl2-like 14 (apoptosis facilitator)	2.0	2.9	—
MRO	Maestro	3.0	3.2	—
NEUROD1	Neurogenic differentiation 1	2.1	0.8	—
NKX2–2	NK2 homeobox 2	2.3	0.4	—
PDK4	Pyruvate dehydrogenase kinase, isozyme 4	2.2	1.6	—
PKHD1	Polycystic kidney and hepatic disease 1	2.3	2.4	—
PTF1A	Pancreas specific transcription factor, 1a	2.4	3.6	—
RNF186	Ring finger protein 186	3.0	4.1	—
SERPINA3	Serine (or cysteine) peptidase inhibitor, clade A, member 3N	3.2	9.8	—
SLC2A2	Solute carrier family 2 (facilitated GLUT), member 2, GLUT2	2.5	2.9	—
TMED6	Transmembrane emp24 protein transport domain containing 6	2.3	4.1	—
VIL1	Villin 1	3.1	3.2	—
CTH	Cystathionase (cystathionine γ-lyase)	2.2	2.9	—
ERBB3	v-erb-b2 Erythroblastic leukemia viral oncogene homolog 3	2.4	0.8	—
FBP1	Fructose-1,6-bisphosphatase 1	2.4	0.9	—
FOXA3	Forkhead box A3	2.6	1.5	—

Continued on p. 1677

Table 1 — Continued

Gene	Description	Fold Change	FDR	Function
HHIP	Hedgehog-interacting protein	2.3	3.2	—
HNF1A	HNF1 homeobox A	2.3	1.6	—
HNF1B	HNF1 homeobox B	2.1	1.6	—
HNF4	Hepatocyte nuclear factor 4, α	3.0	0.8	—
IHH	Indian hedgehog	2.4	1.9	—
KLRK1	Killer cell lectin-like receptor subfamily K, member 1	−2.9	9.8	—
MET	Met proto-oncogene	2.3	1.6	—
Complement activation, alternate pathway				
C3	Complement component 3	3.6	3.2	—
C8A	Complement component 8, α polypeptide	4.6	4.8	—
C8B	Complement component 8, β polypeptide	3.2	9.8	—
CFH	Complement factor H	4.3	5.6	—
CPB2	Carboxypeptidase B2 (plasma)	4.7	4.1	—
CPN1	Carboxypeptidase N, polypeptide 1	2.1	2.9	—
F11	Coagulation factor XI	4.1	3.2	—
KLKB1	Kallikrein B, plasma 1	2.6	9.8	—
MASP2	Mannan-binding lectin serine peptidase 2	2.4	9.8	—
CFI	Complement factor I	4.5	3.2	—
C8G	Complement component 8, γ polypeptide	2.3	3.6	—
C1QTNF5	C1q and tumor necrosis factor related protein 5	−1.5	4.8	—
C1QC	Complement component 1, q subcomponent, C chain	−1.7	9.8	—
C2	Complement component 2	2.1	3.6	—

Genes with differential expression filtered on an FDR of 10% and change ±1.5-fold. Dashes indicate that data are not applicable.

levels remaining increased more than twofold compared with controls (Fig. 1*D*). The levels of several cytokines were less abundant than at e19, suggesting that at PD14, the Th2 activation may be starting to resolve. Surprisingly, by 10 weeks of age, elevated protein levels of Th2 cytokines were no longer observed (Supplementary Table 1), pointing to a limited duration of Th2 activation in IUGR islets.

IUGR Islets Show Immune Cell Invasion and Decreased Vascularity

We next performed immunohistochemistry on whole pancreas from control and IUGR animals at e19 and PD14 using markers for T-cells (CD3) and macrophages (CD68) (Fig. 2*A*). In IUGR fetal islets, islet-associated CD3-positive T-cells and CD68-positive macrophages were increased, and these immune cells persisted to PD14.

Islet function is dependent on vascular density, and protein levels of proangiogenic factors connective tissue growth factor and VEGF were decreased by more than 40% in PD14 IUGR islets (Fig. 1*D*), although VEGF did not reach statistical significance. Similarly, fetal IUGR capillary density was markedly decreased by more than 30% compared with controls. There is a rapid loss of islet vascularity within 24 h of induction of IUGR. PD14 islet capillary density was also decreased 25% in IUGR islets compared with controls (Fig. 2*B* and *C*), consistent with our previous findings of reduced islet vascularity in 1-week-old IUGR animals (22). These results demonstrate the induction of a Th2 immune response in fetal islets that corresponds with loss of islet vascularity that persists until PD14.

Neutralizing IL-4 Rescues Inflammation and Restores Islet Vascularity

We next investigated whether neutralizing IL-4, a key regulatory cytokine of Th2 response, would abrogate the IUGR phenotype. Neonatal IUGR pups were injected daily with a neutralizing IL-4 antibody or PBS for the first 5 days of life. Antibody treatment did not affect weight gain, adiposity, or levels of serum leptin in IUGR animals (Supplementary Fig. 1), demonstrating that increased adiposity in IUGR animals is Th2 independent (Fig. 3*A*). Serum levels of RANTES were significantly elevated in IV animals compared with CV and unchanged by therapy (Fig. 3*A*). This was expected, as RANTES is highly correlated with adiposity (32), and elevated leptin levels from increased adiposity will stimulate RANTES production (33).

Treatment-normalized serum levels of insulin/C-peptide in IIL4-treated animals (Fig. 3*A*). These data suggest that a short-term neonatal treatment with neutralizing IL-4 antibody normalizes the IUGR metabolic milieu. Neutralizing IL-4 also ameliorated the development of systemic inflammation in IUGR animals. Serum levels of MCP1 were reduced 52% in IIL4 animals compared with IV (Fig. 3*A*) and normalized to the level seen in CV- and CIL4-treated

Table 2—PD14 IUGR islets show increases in genes that activate a Th2 immune response and decreases in proangiogenic genes

Gene	Description	Fold Change	FDR	Function
Induction of IL-4/Th2 response and M2 macrophage activation				
TREM2	Triggering receptor expressed on myeloid cells 2	2.1	5.4	Promote Th2 response/M2 macrophages
CLEC10A	C-type lectin domain family 10, member A	1.9	5.4	Promote Th2 response/M2 macrophages
MEFV	Mediterranean fever	−1.6	8.6	Promote Th1 response/prevent M2 macrophage differentiation
IL1RN	IL-1 receptor accessory protein-like 1	−1.6	9.3	Promote Th1 response/prevent M2 macrophage differentiation
IL18	IL-18	−1.7	9.7	Promote Th1 response/prevent M2 macrophage differentiation
CLDN2	Claudin 23	−1.9	9.3	Promote Th1 response/prevent M2 macrophage differentiation
END1	Endothelin 1	−1.9	2.9	Promote Th1 response/prevent M2 macrophage differentiation
ADAM9	ADAM metallopeptidase domain 9 (meltrin γ)	−1.9	9.7	Promote Th1 response/prevent M2 macrophage differentiation
BIRC3	Baculoviral IAP repeat-containing 3	−2.3	8.3	Promote Th1 response/prevent M2 macrophage differentiation
CFTR	Cystic fibrosis transmembrane conductance regulator homolog	−2.3	8.6	Promote Th1 response/prevent M2 macrophage differentiation
A2M	α-2 macroglobulin	−2.4	9.3	Promote Th1 response/prevent M2 macrophage differentiation
CCL19	Chemokine (C-C motif) ligand 19	−2.8	5.9	Promote Th1 response/prevent M2 macrophage differentiation
CCL21	Rattus norvegicus chemokine (C-C motif) ligand 21	−3.1	0	Promote Th1 response/prevent M2 macrophage differentiation
SPIB	Spi-B transcription factor	−3.4	9.7	Promote Th1 response/prevent M2 macrophage differentiation
CD209B	Cd209b	−11.5	9.7	Promote Th1 response/prevent M2 macrophage differentiation
Repression of angiogenesis				
MFAP5	Microfibrillar associated protein 5	2.0	5.4	Antiangiogenic
FUT1	Fucosyltransferase 11 (α (1,3) fucosyltransferase)	1.7	9.7	Antiangiogenic
FGF13	Fibroblast growth factor 13	−1.5	9.7	Proangiogenic
POPDC2	Popeye domain containing 2	−1.5	2.9	Proangiogenic
PRKAA2	Protein kinase, AMP-activated, α 2 catalytic subunit	−1.6	4.5	Proangiogenic
WNT11	Wingless-type MMTV integration site family, member 11	−1.6	8.6	Proangiogenic
DLEU7	Deleted in lymphocytic leukemia, 7	−1.6	8.1	Proangiogenic
FGFR2	Fibroblast growth factor receptor 2	−1.7	8.6	Proangiogenic
CTGF	Connective tissue growth factor	−1.8	11	Proangiogenic
COL4A5	Collagen, type IV, α 5	−2.0	5.5	Proangiogenic
TBX1	T-box 19	−2.8	4.5	Proangiogenic
GREM1	Gremlin 1, cysteine knot superfamily, homolog	−4.2	0	Proangiogenic

Genes with differential expression filtered on an FDR of 10% and change ±1.5-fold.

animals, demonstrating that Th2 inflammation is responsible for the induction of systemic inflammation in postnatal IUGR animals.

Islet capillary density was significantly decreased 43% in IV animals compared with CV (Fig. 3*C* and *D*). Control animals were unaffected, but treatment restored capillary density 187% to that of controls in IIL4 animals and demonstrates that Th2 inflammation is responsible for vascularity loss in IUGR islets.

Histological examination of PD14 IUGR pancreas following neonatal neutralizing IL-4 antibody treatment revealed decreased islet-associated T-cell and macrophage staining (Fig. 3*B*). This suggests that Th2 inflammation is responsible for the recruitment and maintenance of immune cells to IUGR islets. No effect on capillary density or serum cytokine levels was seen in animals treated with nonspecific isotype-controlled IgG antibodies (Supplementary Fig. 2).

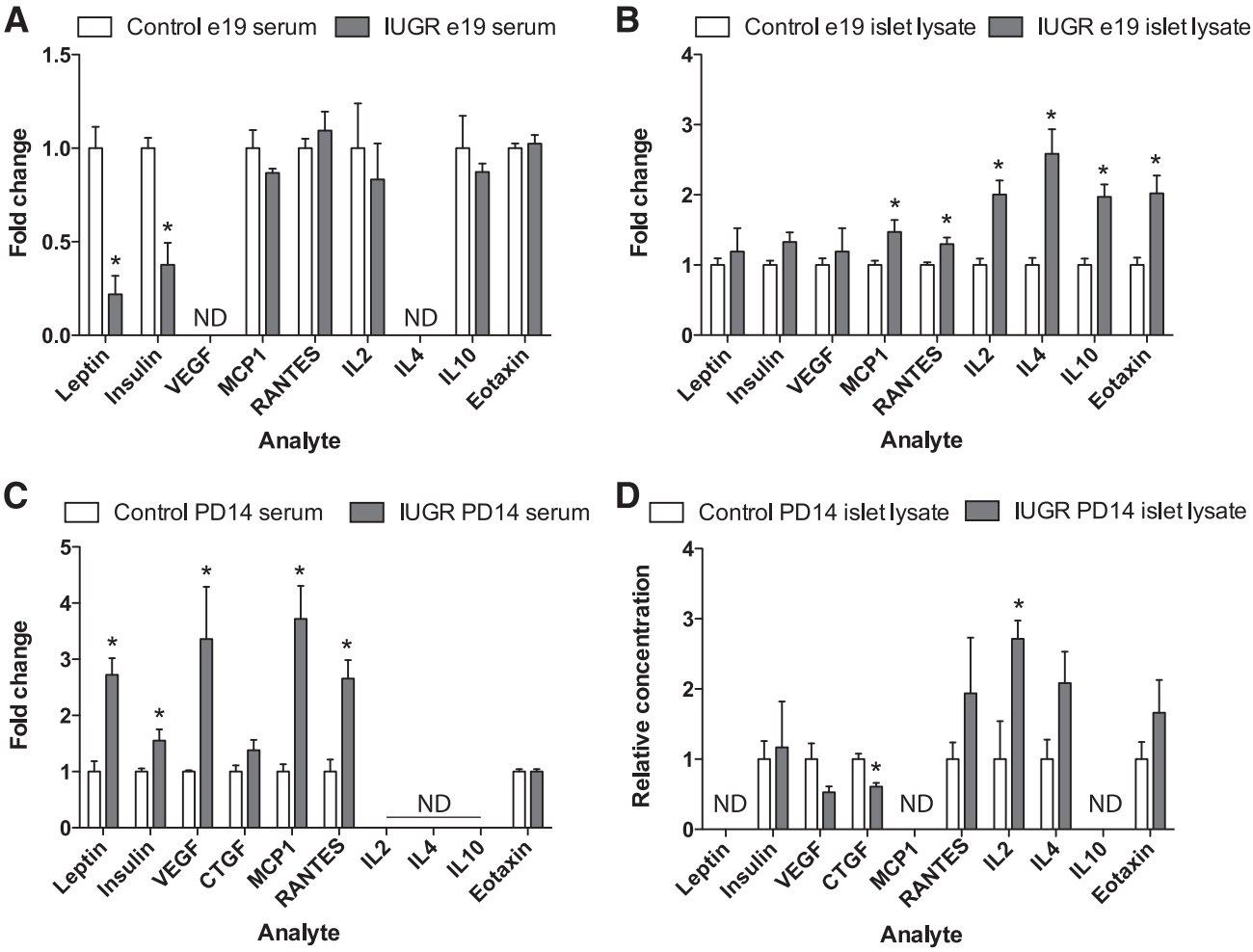

Figure 1—IUGR provokes islet inflammation consistent with Th2 response and M2 macrophage activation in e19 islets. By PD14, IUGR animals develop systemic inflammation, while islet inflammation begins to resolve. Inflammatory cytokine and chemokines were measured by (*A*) Luminex Assay in serum and (*B*) isolated pancreatic islet lysate 24-h postsurgery and in (*C*) serum and (*D*) isolated pancreatic islet lysate from PD14. Data are expressed as fold change compared with controls ± SEM (n = 6–8 measurements/age/group). *, significant difference at $P < 0.05$ versus control; ND, undetectable (analyte was undetectable in tissue); white bars, control; gray bars, IUGR.

Neutralizing IL-4 Restores Glucose-Stimulated Insulin Secretion and Glucose Homeostasis

A key component of IUGR pathophysiology is abnormal β-cell insulin secretion. We isolated islets from 15-week-old animals and measured glucose-stimulated insulin secretion via ramp studies (Fig. 4*A*). The basal rate of insulin release was significantly higher in IV animals compared with CV (Fig. 4*B*), consistent with previous findings of insulin resistance (18). Neutralizing IL-4 therapy restored basal insulin secretion in IIL4 animals to that of CV but had no effect on CIL4 animals. The glucose threshold was similar in all treatment groups. At higher glucose concentrations, the control groups CV and CIL4 had similar maximum insulin release (Fig. 4*C*). Maximum insulin release was decreased 70% in IV compared with CV animals but was restored to that of control animals by neonatal neutralizing IL-4 treatment.

Other cytokines can induce β-cell dysfunction through the generation of oxidative or endoplasmic reticulum stress (34–36). We have previously demonstrated mitochondrial dysfunction and high oxidative stress in IUGR islets, beginning at e19, which persist and intensify over the life of the animal (19). To determine if neutralizing IL-4 antibody therapy improves adult islet function by ameliorating oxidative stress in neonatal islets, we assayed reactive nitrogen species and lipid peroxidation in lysates from 3-week-old treated animals (Fig. 4*D*). Levels of reactive nitrogen species as measured by free nitrate/nitrite levels were over twofold increased in IUGR islets compared with controls. Neutralizing antibody treatment did not have an effect on CIL4-treated animals and failed to rescue high levels in IIL4 animals. Similarly, levels of lipid peroxidation were more than fourfold increased in IV animals compared with CV, but treatment had no effect in IIL4 animals, demonstrating that neutralizing IL-4 therapy restores islet function independently of increased oxidative stress.

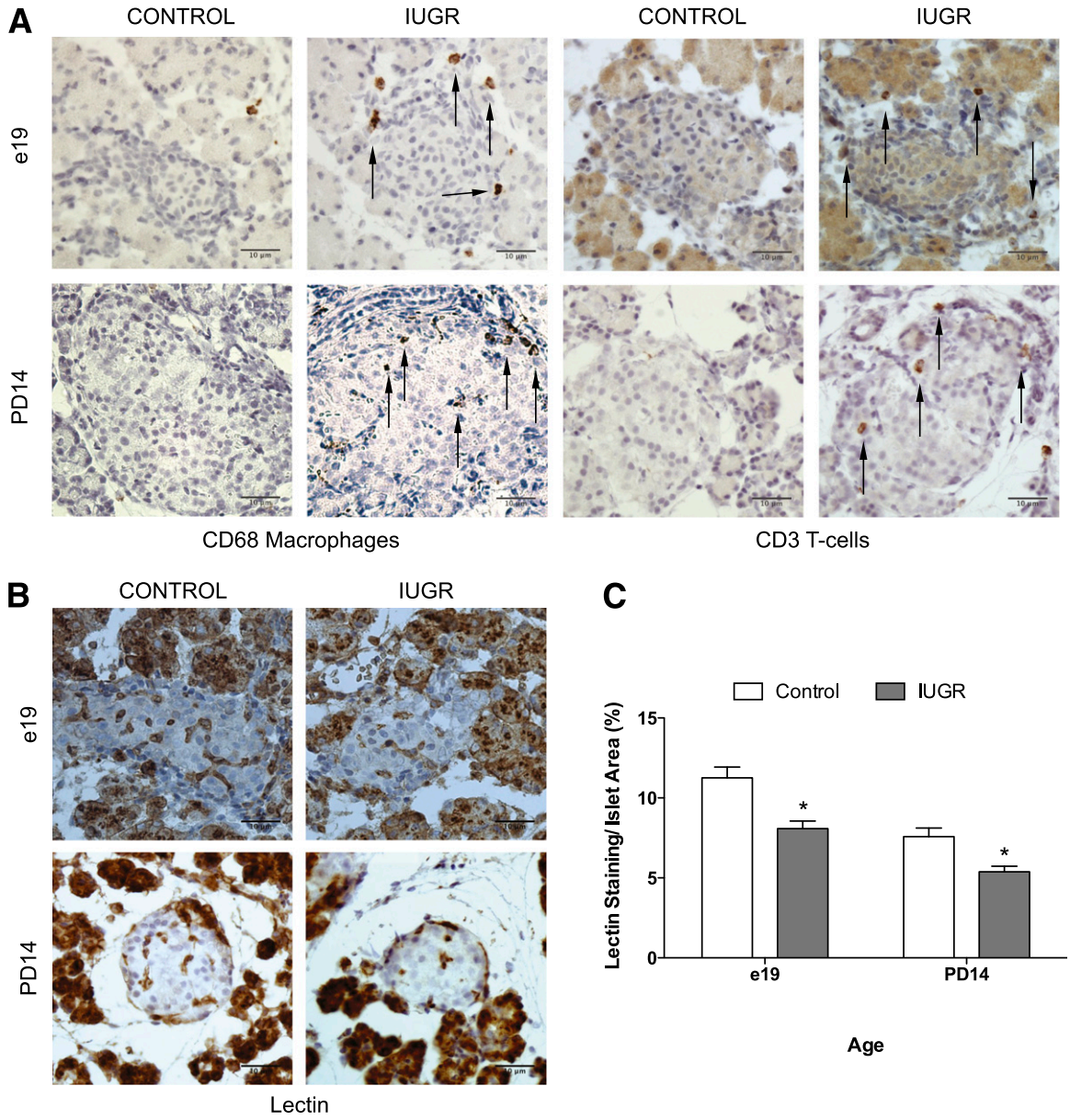

Figure 2—IUGR islets show invasion by T-cells and macrophages and decreased capillary density. *A*: Immunohistochemistry for presence of islet-associated immune cells using antibody to CD68 for macrophages and antibody to CD3 for T lymphocytes at e19 and PD14. The scale bar represents 10 μm in all images. *B* and *C*: Islet capillary density was measured by quantifying the amount of lectin staining per islet in 100 islets. Values are ± SEM (n = 4 measurements/age/group). *, significant difference at $P < 0.05$ compared with control; white bars, control; gray bars, IUGR.

We next measured fasting plasma glucose levels in 8–10-month-old animals (Fig. 5*A*). CV- and CIL4-treated groups had similar glucose levels, whereas fasting glucose levels were significantly elevated in IV animals. Neutralizing IL-4 antibody therapy prevented the development of fasting hyperglycemia in IUGR animals, and levels did not differ from those in CV or CIL4. Fasting C-peptide levels mirrored the glucose levels (Fig. 5*B*) in that CV, CIL4, and IIL4 animals did not differ while IV animals had significantly elevated C-peptide concentrations. Lastly, we measured β-cell mass in these animals (Fig. 5*C*) and found that neutralizing IL-4 antibody therapy prevented loss of β-cell mass in IUGR animals, demonstrating that Th2 inflammation drives β-cell loss in adulthood.

DISCUSSION

The major finding of this study is that IUGR induced by uteroplacental insufficiency provokes a Th2 immune response in the fetal pancreas, which persists until at least PD14. A short treatment course of neutralizing IL-4 antibodies in the newborn period dampens the immune response and restores β-cell function. Thus IUGR invokes a localized Th2 response in the fetal pancreas, leading to the recruitment of T-cells and macrophages. Localized

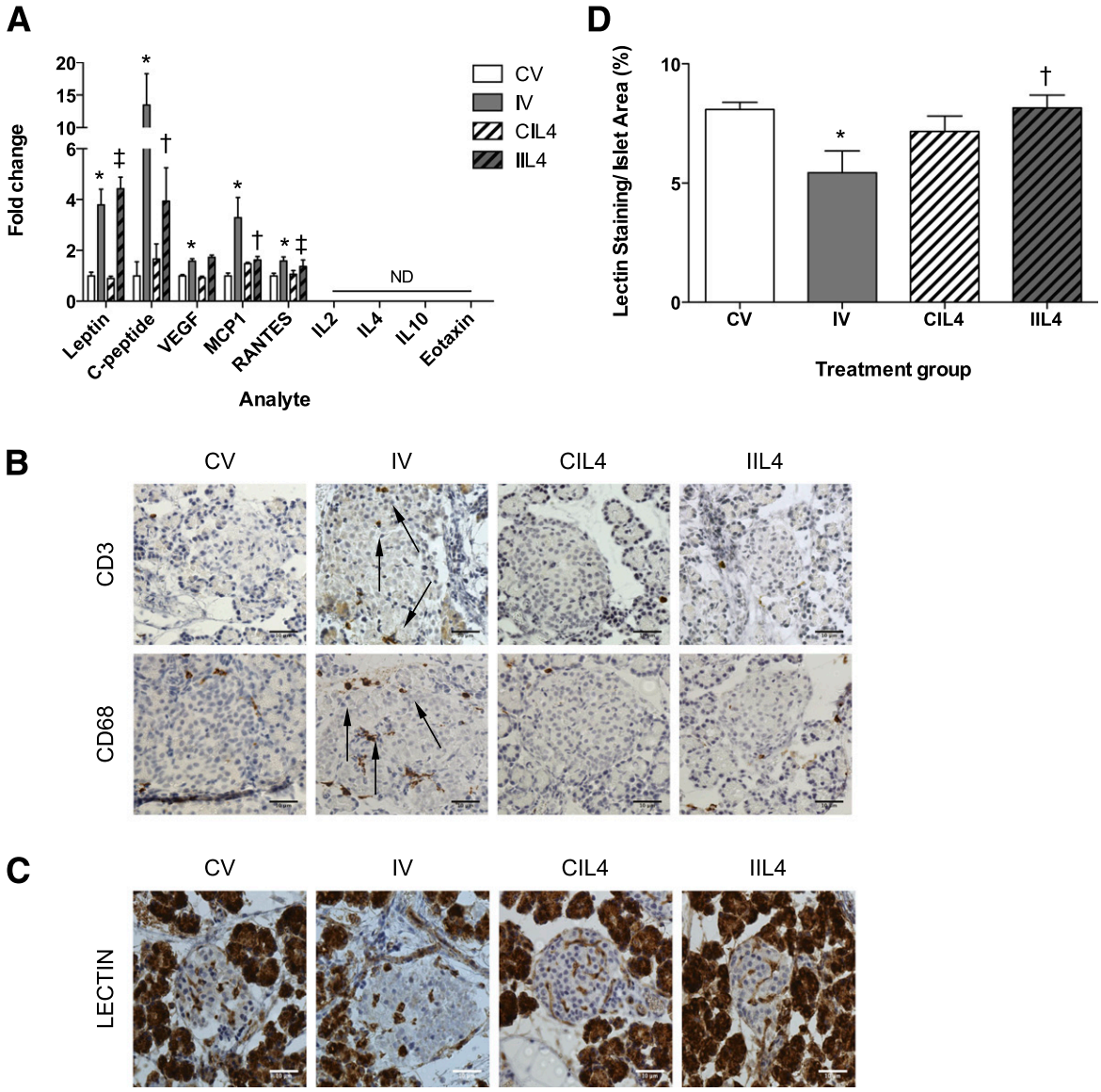

Figure 3—Neutralizing IL-4 treatment rescues inflammation and restores islet capillary density. *A*: Newborn animals were treated with subcutaneous injections of vehicle (PBS) or 1 $\mu g/kg^{-1}$ neutralizing IL-4 antibodies from PD1–6. Inflammatory cytokine and chemokines were measured by Luminex Assay from PD14 serum after treatment. Data are expressed as fold change compared with controls ± SEM (n = 8 measurements/age/group). *B*: Immunohistochemistry for presence of islet-associated immune cells using antibody to CD68 for macrophages and antibody to CD3 for T lymphocytes in PD14 animals following neutralizing IL-4 antibody treatment (n = 6–8 measurements/age; scale bar represents 10 μm in all images). *C* and *D*: Islet capillary density was measured by quantifying the amount of lectin staining per islet in 100 islets/group (n = 4 measurements/group, 100 islets total per group). Values are ± SEM (n = 4 measurements/age/group). *, significant difference at $P < 0.05$ versus CV; ‡, significant difference at $P < 0.05$ versus CIL4; †, significant difference at $P < 0.05$ versus IV; ND, undetectable (analyte was undetectable in tissue); white bars, CV; gray bars, IV; white bars with hatch marks, CIL4; gray bars with hatch marks, IIL4.

inflammation and high IL-4 levels impair insulin secretion and disrupt islet capillary density, leading to vascular insufficiency and reduced β-cell mass. This study is the first to demonstrate that the inflammatory microenvironment of the fetal IUGR pancreas alters β-cell function and disrupts islet vascularity, predisposing IUGR offspring to the development of T2D in adulthood.

Substantial β-cell replication, neogenesis, differentiation, and islet remodeling characterize the neonatal period and are critical for normal adult islet function. The developmental window whereby Th2 inflammation affects this array of structural and molecular changes is important, as it permanently impairs islet function and reduces islet vascularity. IL-4 has been shown to have antiangiogenic effects in vitro, and loss of vascularity is compounded in the presence of IL-10, another Th2 cytokine (37). Functional IL-4 receptors are expressed on both β-cells and endothelial cells, and IUGR likely affects

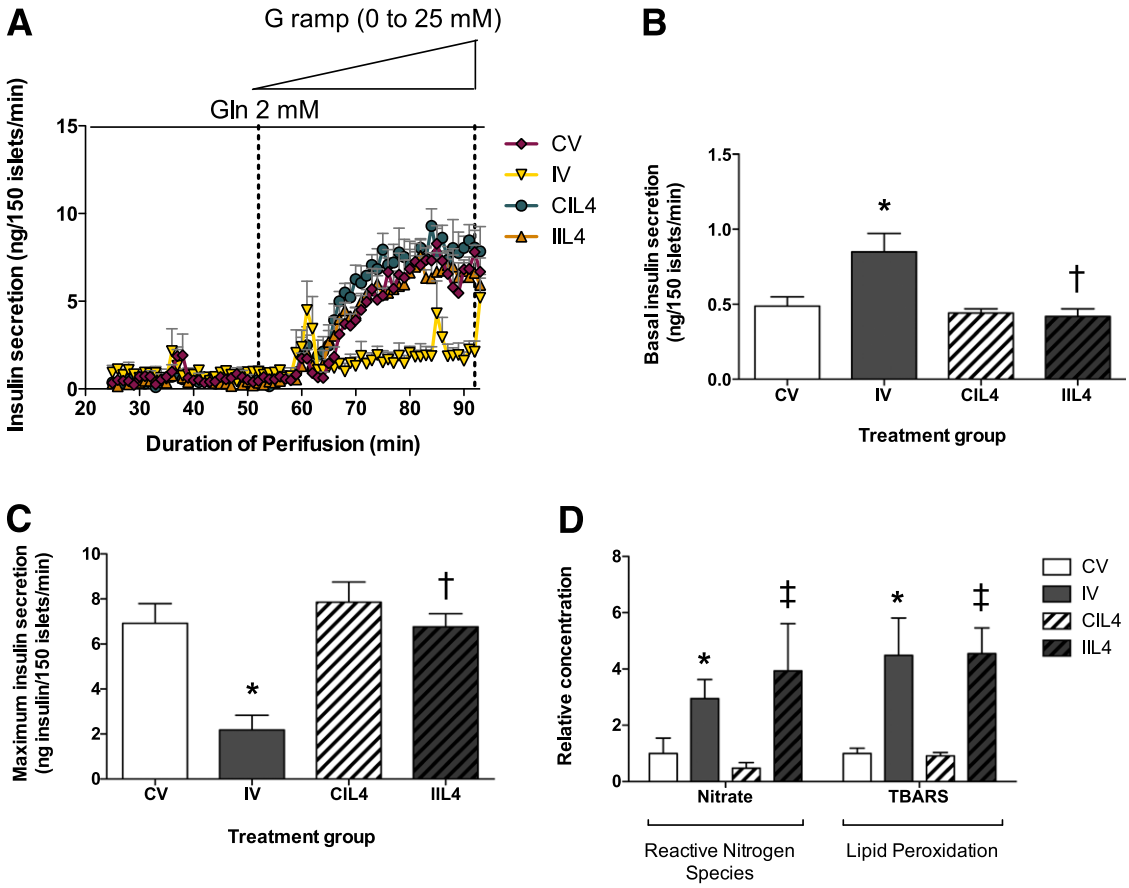

Figure 4—Postnatal neutralizing IL-4 treatment lowers basal insulin release and normalizes maximal insulin secretory capacity. *A*: Isolated islets from 15-week-old animals were perifused in a glucose-free solution with 2 mmol/L glutamine as an alternate fuel source, then glucose concentrations were increased at a flow rate of 0.625 mmol/L glucose/min to a final concentration of 25 mmol/L glucose, and insulin was measured every minute. Values are ± SEM (n = 3 animals/time point/group). *B*: Basal insulin release in the absence of glucose, with 2 mmol/L glutamine. *C*: Maximum insulin release in perifused islets from treatment groups. *D*: Reactive nitrogen species and lipid peroxidation levels in isolated islet lysate from 3-week-old treated animals per total protein content, represented as fold change versus CV. Values are ± SEM (n = 3 animals/time point/group). *, significant difference at $P < 0.05$ versus CV; ‡, significant difference at $P < 0.05$ versus CIL4; †, significant difference at $P < 0.05$ versus IV; Gln, glutamine; G ramp, glucose ramp; white bars, CV; gray bars, IV; white bars with hatch marks, CIL4; gray bars with hatch marks, IIL4.

both cell types through this signaling pathway. In this study, a short course of neonatal neutralizing IL-4 antibody treatment is sufficient to restore islet vascularity, prevent loss of glucose-stimulated insulin secretion, and prevent fasting hyperglycemia in adulthood. To our knowledge, this is the first study to show that a Th2 response may be directly responsible for the initial events that lead to diabetes pathogenesis in IUGR animals.

Evidence of inflammation in diabetes has been seen in many human studies, and rodent models of T2D, as demonstrated by increased levels of IL-1β, MCP1, tumor necrosis factor-α, IL-6, and C-reactive protein, among others. T2D is highly correlated with obesity, and increased adiposity is causally linked to a systemic low-grade subacute inflammatory state (38). Intriguingly, our results demonstrate that inflammation occurs prior to adiposity and begins to resolve as adiposity increases. In human epidemiological studies, subclinical chronic inflammation has been hypothesized to be an important factor in the development of insulin resistance and T2D (39,40). A long-unanswered question in this field is the extent to which T2D and inflammation are triggered in sequence or in parallel. We have made the novel observation that fetal inflammation precedes the adult onset of diabetes and impairs insulin secretion within 24 h of the onset of IUGR. We conclude that adult perturbations in β-cell function are the direct result of fetal inflammation, immune cell infiltration, tissue remodeling, and loss of vascularization.

Other T2D studies have historically shown increases in Th1 cytokines in adipose tissue and systemic and islet activation of the true "proinflammatory" IL-1β pathway. The results are not in conflict, as we show that a brief and localized Th2 activation has profound effects on islet health and function over the life of the animal, even after inflammation is resolved. Moreover, these results point to distinct stages of diabetes progression involving differing inflammatory pathways.

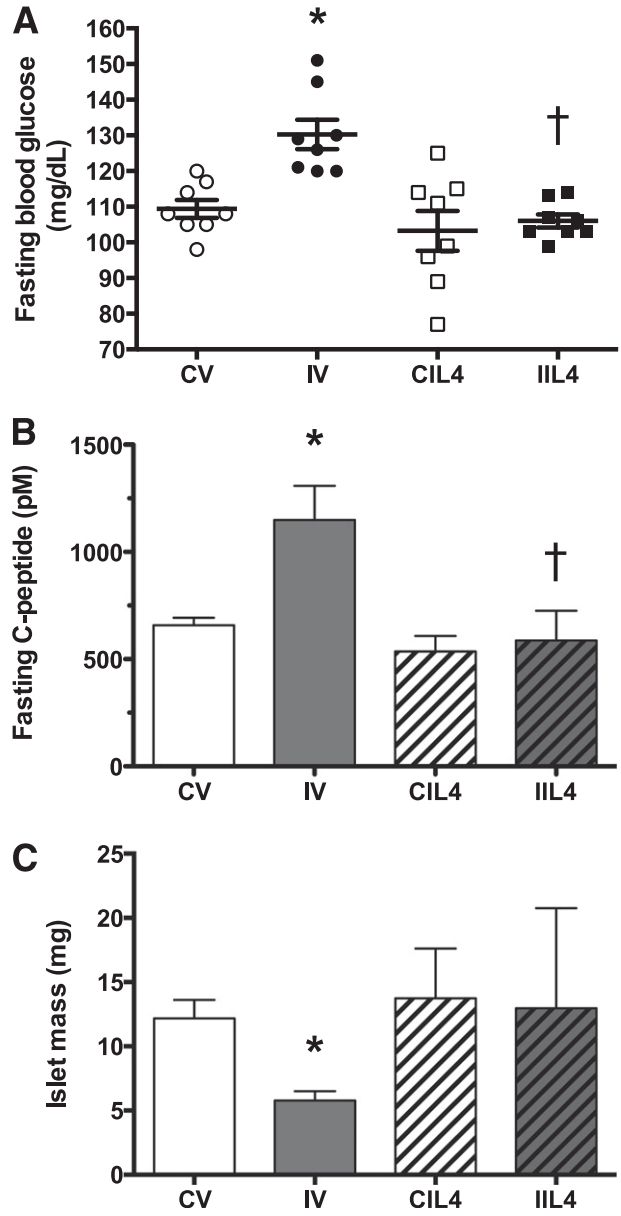

Figure 5—Postnatal neutralizing IL-4 treatment prevents fasting hyperglycemia and loss of β-cell mass in adulthood. Glucose homeostasis and β-cell mass was measured in 6–10-month-old adult animals: (*A*) fasting blood glucose (n = 8 animals/treatment group); (*B*) fasting C-peptide levels (picomolar; n = 8 animals/treatment group; (*C*) islet mass (mg per total pancreas; n = 4 animals/treatment group). Values are ± SEM. *, significant difference at $P < 0.05$ versus CV; †, significant difference at $P < 0.05$ versus IV; white circles, CV; black circles, IV; white squares, CIL4; black squares, IIL4; white bars, CV; gray bars, IV; white bars with hatch marks, CIL4; gray bars with hatch marks, IIL4.

Numerous studies have demonstrated that the predominant maternal immunological cytokine pattern is Th2 (41), which protects against miscarriage. The presence of maternal Th2 cytokines also skews fetal immune responses toward Th2 responses (42). In this study, we show that IUGR activates Th2 responses in fetal tissues. Epidemiological evidence supports the findings of Th2 activation in IUGR, as IUGR has been strongly linked to the postnatal development of asthma, allergies, and hypersensitivity (43,44), all diseases of Th2 activation. We surmise that activation of a fetal Th2 response in utero specifically affects susceptible cells, such as β-cells and alveolar cells, and predisposes to the later development of disease.

In conclusion, these results demonstrate that adult-onset diabetes caused by IUGR is preceded by fetal islet inflammation, which results in immune cell invasion, inflammatory cytokine release, decreased islet vascularity, and increased insulin resistance. Administration of neutralizing IL-4 antibodies at the neonatal stage suppresses inflammatory cytokine levels, normalizes islet vascularity, and permanently restores insulin sensitivity, demonstrating a novel role for Th2 immune responses in T2D instigation and progression. At the neonatal stage, inflammation and vascular changes are reversible and may define an important developmental window for therapeutic intervention to prevent adult-onset diabetes and metabolic syndrome.

Acknowledgments. The authors thank the University of Pennsylvania Molecular Profiling Core for assistance with fetal expression arrays and the Children's Hospital of Philadelphia Pathology Core for assistance with histology profiling.

Funding. This work was supported by National Institutes of Health grant R01-DK-055704 and American Diabetes Association grant 1-11-BS-145 to R.A.S. and National Institutes of Health grants 5T32-HD-00730525 and 1T32-HD-060556 to L.J.J.S. The University of Pennsylvania Radioimmunoassay and Biomarkers Core, Mouse Phenotyping, Physiology and Metabolism Core, and Functional Genomics Core receive support from the Institute for Diabetes, Obesity, and Metabolism National Institutes of Health Research Center grant P30-DK-19525.

Duality of Interest. No potential conflicts of interest relevant to this article were reported.

Author Contributions. L.J.J.S. designed and performed experiments, analyzed data, and wrote the manuscript. C.L. designed and performed experiments and analyzed data. P.-T.D. performed experiments. H.I. designed experiments. G.S.W. and R.A.S. designed experiments, analyzed data, and wrote the manuscript. R.A.S. is the guarantor of this work and, as such, had full access to all the data in the study and takes responsibility for the integrity of the data and the accuracy of the data analysis.

References

1. Simmons RA. Developmental origins of adult disease. Pediatr Clin North Am 2009;56:449–466
2. Gatford KL, Simmons RA, De Blasio MJ, Robinson JS, Owens JA. Review: placental programming of postnatal diabetes and impaired insulin action after IUGR. Placenta 2010;31(Suppl.):S60–S65
3. Homo-Delarche F, Calderari S, Irminger JC, et al. Islet inflammation and fibrosis in a spontaneous model of type 2 diabetes, the GK rat. Diabetes 2006;55:1625–1633
4. Masuyama T, Komeda K, Hara A, et al. Chronological characterization of diabetes development in male Spontaneously Diabetic Torii rats. Biochem Biophys Res Commun 2004;314:870–877
5. Donath MY, Størling J, Maedler K, Mandrup-Poulsen T. Inflammatory mediators and islet beta-cell failure: a link between type 1 and type 2 diabetes. J Mol Med (Berl) 2003;81:455–470

6. Kolb H, Mandrup-Poulsen T. An immune origin of type 2 diabetes? Diabetologia 2005;48:1038–1050
7. Takeda Y, Wakabayashi I. Alteration in lymphocyte population and humoral immune response in type 2 diabetic Goto-Kakizaki rats. Life Sci 2012;90:545–552
8. Bhargava P, Lee CH. Role and function of macrophages in the metabolic syndrome. Biochem J 2012;442:253–262
9. Mantovani A, Sica A, Locati M. New vistas on macrophage differentiation and activation. Eur J Immunol 2007;37:14–16
10. Wynn TA. Fibrotic disease and the T(H)1/T(H)2 paradigm. Nat Rev Immunol 2004;4:583–594
11. Kidd P. Th1/Th2 balance: the hypothesis, its limitations, and implications for health and disease. Altern Med Rev 2003;8:223–246
12. Denney L, Kok WL, Cole SL, Sanderson S, McMichael AJ, Ho LP. Activation of invariant NKT cells in early phase of experimental autoimmune encephalomyelitis results in differentiation of Ly6Chi inflammatory monocyte to M2 macrophages and improved outcome. J Immunol 2012;189:551–557
13. Donath MY, Böni-Schnetzler M, Ellingsgaard H, Halban PA, Ehses JA. Cytokine production by islets in health and diabetes: cellular origin, regulation and function. Trends Endocrinol Metab 2010;21:261–267
14. Donath MY, Shoelson SE. Type 2 diabetes as an inflammatory disease. Nat Rev Immunol 2011;11:98–107
15. Larsen CM, Faulenbach M, Vaag A, et al. Interleukin-1-receptor antagonist in type 2 diabetes mellitus. N Engl J Med 2007;356:1517–1526
16. Cavelti-Weder C, Babians-Brunner A, Keller C, et al. Effects of gevokizumab on glycemia and inflammatory markers in type 2 diabetes. Diabetes Care 2012;35:1654–1662
17. Ramos-Zavala MG, González-Ortiz M, Martínez-Abundis E, Robles-Cervantes JA, González-López R, Santiago-Hernández NJ. Effect of diacerein on insulin secretion and metabolic control in drug-naive patients with type 2 diabetes: a randomized clinical trial. Diabetes Care 2011;34:1591–1594
18. Simmons RA, Templeton LJ, Gertz SJ. Intrauterine growth retardation leads to the development of type 2 diabetes in the rat. Diabetes 2001;50:2279–2286
19. Simmons RA, Suponitsky-Kroyter I, Selak MA. Progressive accumulation of mitochondrial DNA mutations and decline in mitochondrial function lead to beta-cell failure. J Biol Chem 2005;280:28785–28791
20. Stoffers DA, Desai BM, DeLeon DD, Simmons RA. Neonatal exendin-4 prevents the development of diabetes in the intrauterine growth retarded rat. Diabetes 2003;52:734–740
21. Tusher VG, Tibshirani R, Chu G. Significance analysis of microarrays applied to the ionizing radiation response. Proc Natl Acad Sci USA 2001;98:5116–5121
22. Ham JN, Crutchlow MF, Desai BM, Simmons RA, Stoffers DA. Exendin-4 normalizes islet vascularity in intrauterine growth restricted rats: potential role of VEGF. Pediatr Res 2009;66:42–46
23. Carr RM, Patel RT, Rao V, et al. Reduction of TIP47 improves hepatic steatosis and glucose homeostasis in mice. Am J Physiol Regul Integr Comp Physiol 2012;302:R996–R1003
24. Holers VM. The spectrum of complement alternative pathway-mediated diseases. Immunol Rev 2008;223:300–316
25. Krug N, Tschernig T, Erpenbeck VJ, Hohlfeld JM, Köhl J. Complement factors C3a and C5a are increased in bronchoalveolar lavage fluid after segmental allergen provocation in subjects with asthma. Am J Respir Crit Care Med 2001;164:1841–1843
26. Taube C, Thurman JM, Takeda K, et al. Factor B of the alternative complement pathway regulates development of airway hyperresponsiveness and inflammation. Proc Natl Acad Sci USA 2006;103:8084–8089
27. Koistinen HA, Koivisto VA, Andersson S, et al. Leptin concentration in cord blood correlates with intrauterine growth. J Clin Endocrinol Metab 1997;82:3328–3330
28. Setia S, Sridhar MG, Bhat V, Chaturvedula L, Vinayagamoorti R, John M. Insulin sensitivity and insulin secretion at birth in intrauterine growth retarded infants. Pathology 2006;38:236–238
29. Kamei N, Tobe K, Suzuki R, et al. Overexpression of monocyte chemoattractant protein-1 in adipose tissues causes macrophage recruitment and insulin resistance. J Biol Chem 2006;281:26602–26614
30. Joss-Moore LA, Wang Y, Campbell MS, et al. Uteroplacental insufficiency increases visceral adiposity and visceral adipose PPARgamma2 expression in male rat offspring prior to the onset of obesity. Early Hum Dev 2010;86:179–185
31. Morioka T, Asilmaz E, Hu J, et al. Disruption of leptin receptor expression in the pancreas directly affects beta cell growth and function in mice. J Clin Invest 2007;117:2860–2868
32. Mestan K, Ouyang F, Matoba N, Pearson C, Ortiz K, Wang X. Maternal obesity, diabetes mellitus and cord blood biomarkers in large-for-gestational age infants. J Pediatr Biochem 2010;1:217–224
33. Kiguchi N, Maeda T, Kobayashi Y, Fukazawa Y, Kishioka S. Leptin enhances CC-chemokine ligand expression in cultured murine macrophage. Biochem Biophys Res Commun 2009;384:311–315
34. Corbett JA, Lancaster JR Jr, Sweetland MA, McDaniel ML. Interleukin-1 beta-induced formation of EPR-detectable iron-nitrosyl complexes in islets of Langerhans. Role of nitric oxide in interleukin-1 beta-induced inhibition of insulin secretion. J Biol Chem 1991;266:21351–21354
35. Welsh N, Eizirik DL, Bendtzen K, Sandler S. Interleukin-1 beta-induced nitric oxide production in isolated rat pancreatic islets requires gene transcription and may lead to inhibition of the Krebs cycle enzyme aconitase. Endocrinology 1991;129:3167–3173
36. Arnush M, Heitmeier MR, Scarim AL, Marino MH, Manning PT, Corbett JA. IL-1 produced and released endogenously within human islets inhibits beta cell function. J Clin Invest 1998;102:516–526
37. Hong KH, Cho ML, Min SY, et al. Effect of interleukin-4 on vascular endothelial growth factor production in rheumatoid synovial fibroblasts. Clin Exp Immunol 2007;147:573–579
38. Mathis D, Shoelson SE. Immunometabolism: an emerging frontier. Nat Rev Immunol 2011;11:81
39. Sjöholm A, Nyström T. Inflammation and the etiology of type 2 diabetes. Diabetes Metab Res Rev 2006;22:4–10
40. Imai Y, Dobrian AD, Morris MA, Nadler JL. Islet inflammation: a unifying target for diabetes treatment? Trends Endocrinol Metab 2013;24:351–360
41. Wegmann TG, Lin H, Guilbert L, Mosmann TR. Bidirectional cytokine interactions in the maternal-fetal relationship: is successful pregnancy a TH2 phenomenon? Immunol Today 1993;14:353–356
42. Prescott SL, Macaubas C, Holt BJ, et al. Transplacental priming of the human immune system to environmental allergens: universal skewing of initial T cell responses toward the Th2 cytokine profile. J Immunol 1998;160:4730–4737
43. Duijts L. Fetal and infant origins of asthma. Eur J Epidemiol 2012;27:5–14
44. Steffensen FH, Sørensen HT, Gillman MW, et al. Low birth weight and preterm delivery as risk factors for asthma and atopic dermatitis in young adult males. Epidemiology 2000;11:185–188